BJPS

Brazilian Journal of
Pharmaceutical Sciences

http://dx.doi.org/10.1590/s2175-97902022e19731

Article

# Poloxamer-enhanced solubility of griseofulvin and its related antifungal activity against *Trichophyton* spp.

**Vanessa Pittol[1*], Kleyton Santos Veras[1], Samuel Kaiser[1], Letícia Jacobi Danielli[2], Alexandre Meneghello Fuentefria[3], George González Ortega[1]**

*[1]Laboratory of Galenic Development, Pharmacy Faculty, Federal University of Rio Grande do Sul, Porto Alegre, RS, Brazil, [2]Laboratory of Pharmacognosy, Pharmacy Faculty, Federal University of Rio Grande do Sul, Porto Alegre, RS, Brazil, [3]Laboratory of Applied Mycology, Pharmacy Faculty, Federal University of Rio Grande do Sul, Porto Alegre, RS, Brazil*

Poorly water-soluble drugs, such as the antifungal drug griseofulvin (GF), exhibit limited bioavailability, despite their high membrane permeability. Several technological approaches have been proposed to enhance the water solubility and bioavailability of GF, including micellar solubilization. Poloxamers are amphiphilic block copolymers that increase drug solubility by forming micelles and supra-micellar structures via molecular self-association. In this regard, the aim of this study was to evaluate the water solubility increment of GF by poloxamer 407 (P407) and its effect on the antifungal activity against three *Trichophyton mentagrophytes* and two *T. rubrum* isolates. The GF water solubility profile with P407 revealed a non-linear behavior, well-fitted by the sigmoid model of Morgan-Mercer-Flodin. The polymer promoted an 8-fold increase in GF water solubility. Fourier-transform infrared (FT-IR) spectroscopy, differential scanning calorimetry (DSC), and 2D nuclear magnetic resonance (NMR Roesy) spectroscopy suggested a GF-P407 interaction, which occurs in the GF cyclohexene ring. These results were supported by an increase in the water solubility of the GF impurities with the same molecular structure. The MIC values recorded for GF ranged from 0.0028 to 0.0172 mM, except for *T. mentagrophytes* TME34. Notably, the micellar solubilization of GF did not increase its antifungal activity, which could be related to the high binding constant between GF and P407.

**Keywords:** Griseofulvin. Poloxamer 407. Micellar solubilization. Drug-polymer interaction. Antifungal activity.

## INTRODUCTION

Aqueous solubility is an essential property for drug formulation and targeted activity and thus represents a major challenge for technological development (Takagi *et al.*, 2006; Kawabata *et al.*, 2011; Buckley *et al.*, 2013; Khadka *et al.*, 2014). The Class II drugs of the Biopharmaceutics Classification System can preclude the development of effective dosage forms owing to their poor solubility in water and biological fluids (Aly *et al.*, 1994; Amidon *et al.*, 1995; Fujioka *et al.*, 2007; Noomen *et al.*, 2008). Griseofulvin (GF) (Figure 1), a fungistatic drug of choice for the treatment of dermatomycoses such as tinea capitis, especially infections caused by the genera *Epidermophyton*, *Trichophyton,* and *Microsporum*, is an example of such drug (Finkelstein, Amichai, Grunwald, 1996; Shishu, Aggarwal, 2006; Aggarwal, Shishu, Khurana, 2013; Gupta *et al.*, 2018).

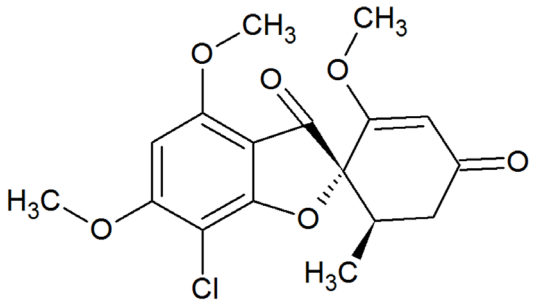


**Figure 1 –** Chemical structure of griseofulvin (GF).

***Correspondence:** V. Pittol. Faculdade de Farmácia. Universidade Federal do Rio Grande do Sul. Av. Ipiranga, 2752/606, Porto Alegre/RS, Brasil, 90610-000. Email: nessa_pittol@hotmail.com. ORCID: https://orcid.org/0000-0003-3049-7348

Several pharmaceutical approaches have been adopted to increase the aqueous solubility and bioavailability of GF, such as self-emulsifying drug delivery systems, solid dispersions, cocrystals, and cyclodextrin complexation (Dhanaraju *et al*., 1998; Arida, Al-Tabakha, Hamoury, 2007; Aitipamula *et al*., 2012; Cheng *et al*., 2015). Micellar solubilization by polymers is another alternative for overcoming problems that arise from poorly soluble drugs and hydrophobic molecules, including drug formulation and bioavailability (Lee *et al*., 2008; Liveri *et al*., 2012). Poloxamers are triblock copolymers consisting of ethylene oxide (EO) and propylene oxide (PO) units in an amphiphilic arrangement (Rowe, Sheskey, Owen, 2005; Dumortier *et al*., 2006). Their structure enables self-association from simple to more complex micelles with hydrophobic (PO) and hydrophilic (EO) domains (Kabanov, Alakhov, 2002). Poloxamer 407 (P407) is one of the most studied poloxamers due to its water solubility and excellent capacity to interact with hydrophobic drugs (Lau *et al*., 2004; Rowe, Sheskey, Owen, 2005; Dumortier *et al*., 2006). Studies on the micellar solubilization of GF, including di- and triblock copolymers, have been presented in the literature; however, these studies are restricted to technological issues, with no experimental evidence of the reflex on antifungal activity (Rekatas *et al*., 2001; Ribeiro *et al*., 2009; Oliveira *et al*., 2011). The formation of polymer micelles by P407 alone and its effect on GF aqueous solubility and antifungal activity are yet to be explored.

The present work aimed to evaluate GF solubilization using P407 and their reflex on the antifungal activity of GF against *Trichophyton mentagrophytes* and *Trichophyton rubrum* isolates.

## MATERIAL AND METHODS

### Material

Griseofulvin (98% purity) and acetone-$d_6$ were purchased from Sigma Aldrich (St. Louis, MO, USA). Poloxamer 407 (Pluronic® F127) was kindly provided by BASF (Ludwigshafen am Rhein, Germany). Acetonitrile (Merck Millipore, Darmstadt, Germany), formic acid (Tedia, Fairfield, USA), and ultrapure water obtained from a Milli-Q® system (Millipore Merck, Darmstadt, Germany) were used for the mobile phase in LC analysis. Sterilizing filters (0.22-µm membrane) were obtained from Sartorius (Goettingen, Germany). For the antifungal assay, RPMI 1640 culture medium and potato dextrose agar were purchased from Sigma Aldrich.

### Quantification and characterization by HPLC-PDA

GF quantification was performed using an HPLC instrument (Prominence, Shimadzu, Kyoto, Japan) equipped with an FCV-AL 10 system controller, LC-20 AT pump, SIL-20 A autosampler, and a photodiodo array detector (PDA) SPD-M20A. The stationary phase was a Kinetex® Phenomenex C18 100A column (150 × 4.6 mm ID, 5 µm) coupled with a SecurityGuard ULTRA Phenomenex C18 guard column (4.6 mm ID, sub-2 µm). An isocratic system was employed, with a mixture of 0.1% (v/v) formic acid in water (A) and acetonitrile (B) (65:35%, v/v) as the mobile phase. The flow rate (1.1 mL/min) and temperature (35 ± 1 °C) were kept constant throughout the analysis, and absorption was detected at 290 nm. All samples were appropriately diluted with mobile phase and filtered through a 0.45-µm membrane (Millipore®, Merck Millipore, Darmstadt, Germany). The method was previously validated according to ICH guidelines (data not shown).

### Solubilization assay

P407 aqueous dispersions in the 0.02-4.8 mM concentration range were prepared and maintained overnight at 10 °C. Separately, a GF excess above water saturation was added to the dispersions. Thereafter, the mixtures were stirred magnetically for 24 h at 37 ± 1 °C (MULTISTIRRER Velp, Usmate, MB, Italy). The samples were centrifuged for 20 min at 3.600 G, and the supernatant was filtered through a 0.45-µm membrane. An aliquot of each solution was diluted with the mobile phase for subsequent analysis by HPLC-PDA. The intrinsic solubility of GF was determined using ultrapure water

under the same experimental conditions. The impurities present in GF samples were analyzed by HPLC and their solubilization profiles were recorded. All analyses were performed in triplicate.

## Physicochemical characterization

### *Fourier-transform infrared spectroscopy (FT-IR)*

The FT-IR spectra of GF, P407, and GF-P407 physical mixture (1:1, w/w) were recorded in the scanning range of 4000 – 600 $cm^{-1}$, using a resolution of 4 $cm^{-1}$ and 40 accumulations (Spectrum BX FTIR, PerkinElmer, Waltham, USA).

### *Differential scanning calorimetry (DSC)*

Thermograms were recorded using a Shimadzu DSC-60 calorimeter, and data analysis was performed using TA Analysis Software (Shimadzu, Kyoto, Japan). Accurately weighed amounts of approximately 1 – 2 mg of GF, P407, and GF-P407 physical mixture (1:1, w/w) were analyzed in crimped aluminum pans. The operating conditions were a heating rate of 10 °C/min (25 to 250 °C) and a dynamic nitrogen atmosphere of 50 mL/min.

### *Nuclear magnetic resonance spectroscopy (NMR) studies*

One-dimensional $^{1}H$ NMR and homonuclear 2D-Roesy spectra were recorded using a Bruker 400 MHz spectrometer (Bruker, USA) operating at 400 MHz and room temperature. The data were processed using MestReNova® 6.0 software (Mestrelab Research©, Spain). Sample solutions of GF, P407, and GF-P407 physical mixture (3:1, w/w) were prepared using acetone-$d_6$.

### *Analysis by Zetasizer*

The particle size and polydispersity index (PDI) of P407, alone and associated with GF, were determined by photon correlation spectroscopy. Zeta potential (ζ) and conductivity were measured by electrophoretic mobility (Zetasizer 3000HS, Malvern Instruments, Malvern, England). Samples were prepared in the same concentrations and experimental conditions described in the solubilization assay and analyzed at 37 °C.

### *Multivariate analysis*

Hierarchical clusters (HCA) and principal component (PCA) analyses of particle size, PDI, ζ potential, conductivity, GF solubilization, and polymer concentration were performed using MINITAB® 16 software (State College, PA, USA). The number of components was determined according to the magnitude of the eigenvalues following the Mahalanobis distance. Each variable was evaluated as per the set of data obtained in triplicate on three different days. For the non-unimodal samples, the particle size of the major population (> 90%) was selected for analytical purposes.

## Fungal susceptibility tests

### *Microorganisms*

The isolates of *Trichophyton mentagrophytes* (TME16, TME34, and TME40) and *Trichophyton rubrum* (TRU43, TRU51) were obtained from the culture collection of the Laboratory of Applied Mycological Research, Federal University of Rio Grande do Sul, Porto Alegre, Brazil. Fungal inocula were prepared according to the Clinical Laboratory Standard Institute protocol (M38-A2 document, CLSI, 2008). After incubation, the conidia suspension was prepared, and the concentration was adjusted in a counting chamber for $1x10^3$ – $3x10^3$ CFU/mL.

### *Work samples*

Samples of the GF and GF-P407 mixtures at different polymer concentrations (0.04, 0.8, 1.6, 2.4, and 4.8 mM) were prepared as described in the solubilization assay. All work samples were prepared under laminar flow aseptic conditions and sterilized by filtration through a 0.22-µm membrane. GF alone was solubilized with ultrapure water, according to the

intrinsic solubility assay, and filtered to eliminate the particles that were not soluble.

*Minimum inhibitory concentration test (MIC)*

The minimum inhibitory concentration values of each sample were determined by the microdilution broth method according to the Clinical Laboratory Standard Institute protocol (M38-A2 document - CLSI, 2008), with modifications. GF and GF-P407 solutions were tested against the isolates of *T. mentagrophytes* and *T. rubrum* at concentrations ranging from $5.56x10^{-5}$ – 0.011 mM and $1.95x10^{-4}$ – 0.039 mM of GF, respectively. For *T. mentagrophytes* (TME 34), the GF-P407 sample was tested in the concentration range of $3.89x10^{-4}$ – 0.097 mM of GF and the plates were incubated at 32 °C for five days. The MIC was defined as the lowest concentration of GF where the tested isolate did not demonstrate visible growth. The assay was performed in triplicate for each sample on three different days. The viability of fungal growth, sterility of the culture medium and samples, and the effect of the sample containing only polymer were used as controls.

## RESULTS AND DISCUSSION

### Solubility assay

The solubilization assay data revealed an approximately 8-fold increase in the solubility of GF in the highest P407 concentration. The GF-P407 solubilization profiles appeared as a sigmoid-shaped curve and were better fitted by the Morgan-Mercer-Flodin mathematical model ($y = [ab + cx^d]/[b + x^d]$) but with a discrete regression coefficient ($R^2 = 0.90$) (Figure 2). Notably, sigmoid-shaped curves are not always common in drug solubilization profiles. For instance, the GF solubilization disagrees with that reported for felodipine under similiar experimental conditions, in which the solubilization occurred as a linear function of P407 concentration (Lee *et al.*, 2008). In addition, the GF-P407 sigmoid-shaped curve described above was unrelated to any experimental conditions applied in this work, as confirmed after five replications at different days. This might be linked to the formation and coexistence of globular, lamellar, cylindrical, hexagonal, and cubic micellar arrangements, after spontaneous self-association of the single poloxamer molecules (Lawrence, 1994; Alexandridis, Olsson, Lindman, 1998; Mortensen, 2001; Kabanov, Alakhov, 2002). The self-association of the poloxamer in different structures can occur at low concentrations, below its critical micelle concentration (CMC), depending on the surrounding temperature (Lin, Alexandridis, 2002; Lee *et al.*, 2008; Ren *et al.*, 2015). In fact, there is no consensus on the P407 CMC value being reported from 0.18% (25 °C) to 0.01% (37 °C). As a rule, the more complex the micelle structure, the higher the drug solubilization (Kabanov, Alakhov, 2002). In addition, a more intricate picture emerges following the addition of a solute that can contribute to a high structural polymorphism and the coexistence of distinct molecular arrangements in a dynamic manner. Thus, the coexistence of these structures, different stages of self-assembly with the addition of the copolymer, and the potential interaction of the drug could explain the decrease in GF solubility in some P407 concentrations (Alexandridis *et al.*, 1994; Ivanova, Lindman, Alexandridis, 2000a; Ivanova, Lindman, Alexandridis, 2000b; Kabanov, Alakhov, 2002; Ren *et al.*, 2015).

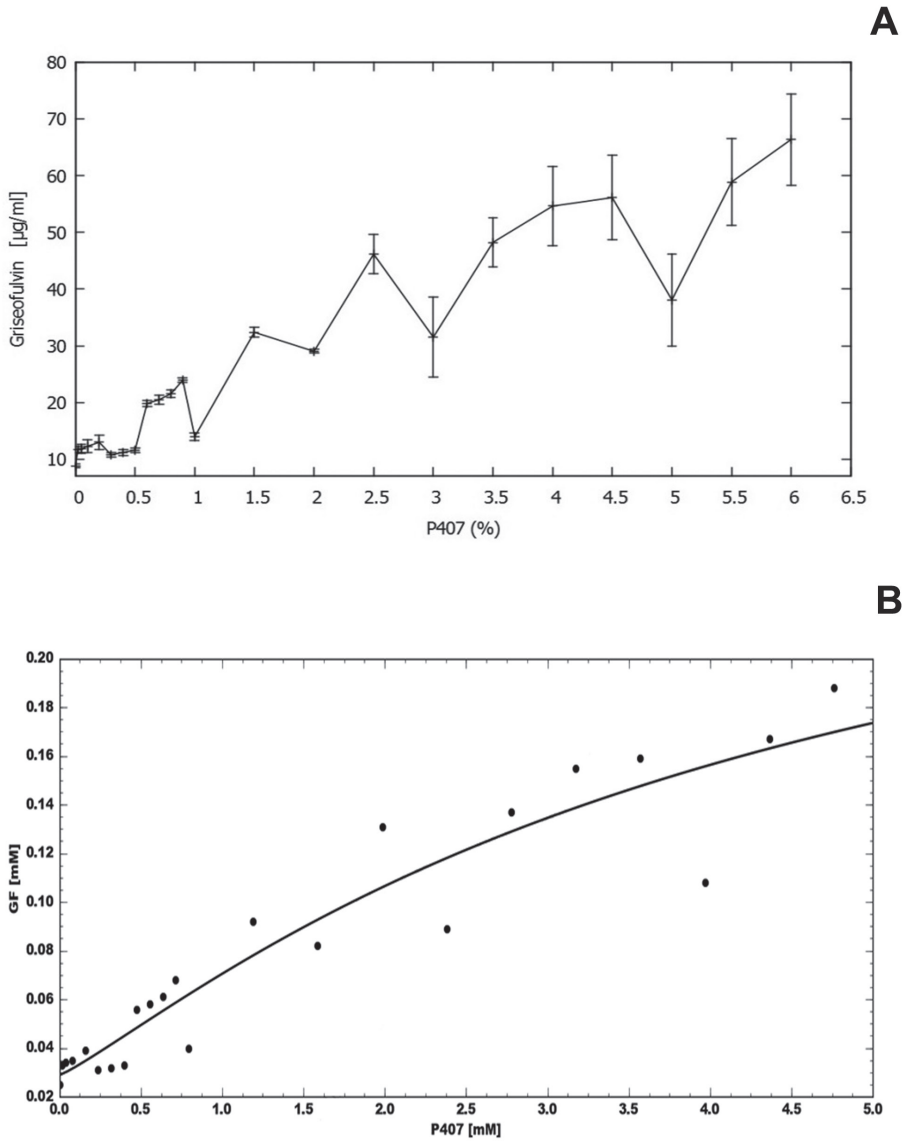


**Figure 2 -** Curve of GF solubilized (µg/mL) versus P407 concentration (%) (A); and the curve of GF solubilized (mM) versus P407 concentration (mM) adjusted by the Morgan-Mercer-Flodin model (CurveExpertPro-2.6.3) (B).

## FT-IR

The potential interactions between GF and P407 were investigated by FT-IR analysis by comparing the respective absorption spectra, considering specific functional groups of GF and P407 alone, and the GF-P407 physical mixture (1:1, w/w). The choice of this ratio between GF and P407 was based on studies of drug-excipient compatibility for maximizing the probability of observing any GF-P407 interaction.

The GF spectrum showed characteristic bands at 2945 $cm^{-1}$ (C=C─H stretching), 1704 $cm^{-1}$ and 1658 $cm^{-1}$ (stretching of the carbonyl group of benzofuran and cyclohexene, respectively), 1614 $cm^{-1}$ and 1584 $cm^{-1}$ (aromatic C=C), 1210 $cm^{-1}$ (C─O stretching attached in ring), 1135 $cm^{-1}$ (C=C─O stretching), and 800 $cm^{-1}$ (aromatic C─H) (Figure 3A). The P407 spectrum showed characteristic bands at 2881 $cm^{-1}$ (aliphatic C─H) and 1100 $cm^{-1}$ (C─O stretching) (Figure 3B) (Garg, Sachdeva, Kapoor, 2013).

The spectrum of the GF-P407 physical mixture (Figure 3C) presented almost all characteristic bands of both substances, except the GF band at 2945 $cm^{-1}$. In addition, evident intensity and shape changes were recorded, mainly the decreased intensity of the GF bands at 1210 and 1135 $cm^{-1}$ and the shape and intensity change of the P407 band at 1100 $cm^{-1}$. These results suggest the involvement of the proton of the cyclohexene ring of GF in the molecular interaction between GF and P407.

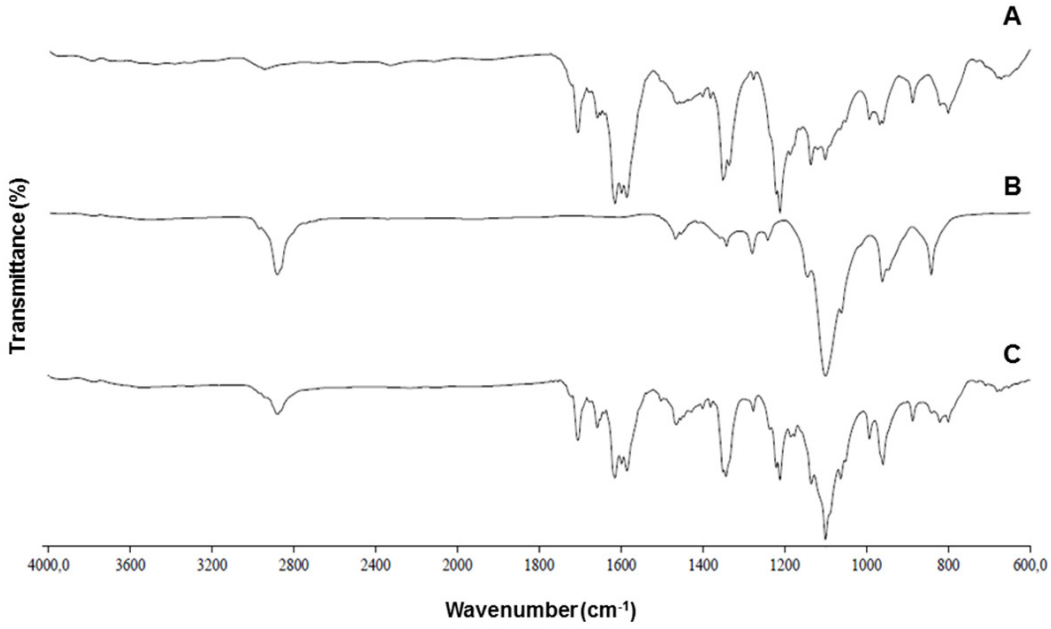


**FIGURE 3 –** Fourier-transform infrared (FT-IR) spectrum of (A) GF; (B) P407, and (C) GF-P407 physical mixture (1:1, w/w).

## DSC

The DSC curves of GF, P407, GF-P407 physical mixture (1:1, w/w), and the reanalysis after cooling of the previously melted physical mixture are shown in Figure 4. Both the GF (A) and P407 (B) curves matched the published data (Feng, Pinal, Carvajal, 2008; Garg, Sachdeva, Kapoor, 2013), showing endothermic peaks at 218 and 52 °C, respectively.

In addition, the curve of the GF-P407 physical mixture (C) revealed a slight displacement of the endothermic peak of P407 and the complete disappearance of the GF peak. This implies a clear modification of the crystalline structure of GF linked to a feasible molecular interaction between GF and P407; however, it can also be associated with the solubilization of GF in the mass of a previously melted polymer. The same behavior was observed in the DSC analysis of solid dispersions composed of felodipine and P407 (Kim *et al.*, 2006). The reanalysis of the GF-P407 physical mixture (D) reinforced the postulation of a potential solubilization of GF in the polymer, taking into account the lack of any thermal variation event in the same temperature range.

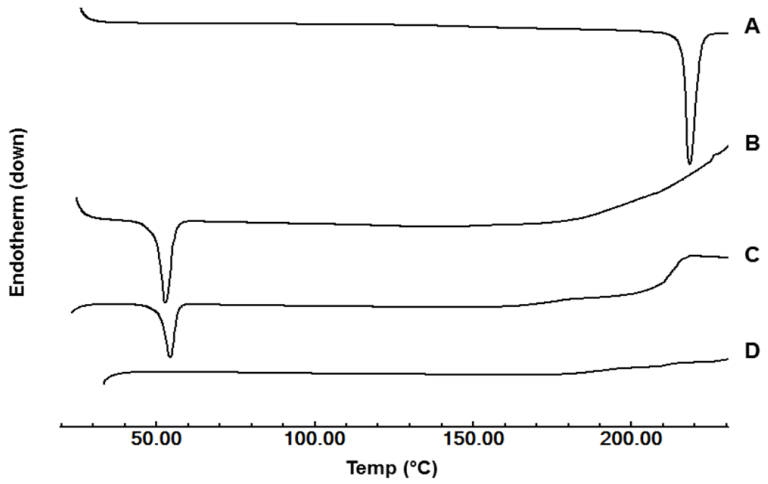


**FIGURE 4 -** DSC curves of (A) GF; (B) P407; (C) GF-P407 physical mixture (1:1, w/w), (D) reanalysis of the physical mixture under the same experimental conditions.

## NMR studies

Homonuclear 2D-Roesy is commonly used to elucidate the intermolecular interactions between two or more substances. The data obtained herein for the GF-P407 mixture did not enable us to draw a concrete conclusion regarding the interaction region. The Roesy spectrum showed a region of interaction that involved the proton of the GF cyclohexene ring (5.6 ppm) and some protons of P407 at the chemical shift region of 3.6 – 3.8 ppm. This result suggests that the interaction occurs with the $CH_2$ group of the poloxamer EO part, indicating that GF molecules are not exclusively located in the micelles. However, the high proximity of the signals of both substances in this region interferes with the ideal visualization of the phenomenon and exact confirmation of the protons involved in the process. Another interference could be the organic solvent choice owing to the low GF solubility, which prevents the use of deuterium oxide in the evaluation (Supplementary Material).

## Analysis by Zetasizer

The initial concentrations of P407 (0.016 mM, 0.04 mM, and 0.08 mM), alone or combined with GF, showed bimodal and trimodal particle size populations. The polydispersity index ranging from 0.5 to 0.6 corroborated a clear heterogeneity among the particle size population. The population with the smallest particle size (approximately 2 nm) was assigned to small structures as polymer chains. Particles of intermediate size (25 nm) predominated over other populations and were ascribed to single micellar structures. Conversely, those with the largest size (100 nm) to more complex structures or the polymer aggregates did not completely disperse. However, a tendency toward a unimodal distribution accompanied by a decrease in PDI values (between 0.1 and 0.2) was observed after the P407 concentration was increased. Thus, particle size remained in the range of 20 to 30 nm, and no direct correlation was observed between the increase in P407 concentration and particle size. The obtained data reflected those previously reported by Chiappetta *et al.* (2011), who observed a similar behavior and the presence of micelle structures of approximately 20 nm in the P407 dispersions. The Zetasizer analysis carried out after GF addition showed similar particle size distribution and PDI, demonstrating that both variables were not affected by the presence of GF. The (zeta) ζ potential of the P407 dispersions varied from − -20 to -5 mV, according to the increase in P407 concentration, which may be due to the formation of micelle arrangements in different ways. The decrease in the ζ potential values indicates a higher aggregation tendency of the polymer molecules and lower stability of the polymeric micelles (Sezgin, Yüksel, Baykara, 2006; Ghaffari *et al.*, 2011; Suksiriworapong *et al.*, 2014). The GF-P407 dispersions showed the same behavior, but varied from -8 mV to -2 mV. Such finding suggests that GF molecules are interacting with the P407 micelles,

in some extension, at least. Furthermore, the instability of the system indicated by the lower ζ potential values could explain the sigmoid profile of GF solubilization. The conductivities of the P407 dispersions and GF-P407 dispersions were very similar, ranging from 0.05 – 0.18 μS/cm to 0.02 – 0.15 μS/cm, respectively. This discrete conductivity value is associated with the nonionic nature of the poloxamer and can be ascribed to the increase in P407 concentration.

## Multivariate analysis

To clarify the potential correlations between the variable P407 concentration, particle size, PDI, ζ potential, conductivity, and amount of solubilized GF, HCA and PCA analyses were performed. Both multivariate methods revealed two clusters (Figure 5A), with approximately 90.8% of the variability explained by the factor extractions, PC1 and PC2 (Figure 5B). The two groups demonstrated an antagonistic relationship, as displayed by the separation between both clusters and the location of the descriptive vectors in opposing camps. The first cluster included polymer concentration, conductivity, and solubilized GF. Thus, a high similarity between these variables can be inferred, confirming the correlation between the increase in P407 concentration and the amount of solubilized GF and the conductivity. The second cluster was comprised of particle size, PDI, and ζ potential. Thus, the three measures showed clear opposition for the first cluster, indicating that there is no linear relationship between the variation in these values and an increase in P407 concentration and GF solubility. Within the second cluster, a high similarity existed between particle size and PDI, which was expected as these measures are correlated. A further multivariate analysis omitting the solubilized GF data was carried out to infer its effect on GF-P407 behavior; however, no tangible changes were observed in the dendrograms described below (Figure 6A). Briefly, the variability explained by PC1 and PC2s remained at 93.3% (Figure 6B), and slight changes in the angle between some vectors were demonstrated, without characterizing significant changes. Thus, multivariate analysis revealed a correlation between the variables of interest but did not allow a clear visualization of the role of GF in this dynamic system.

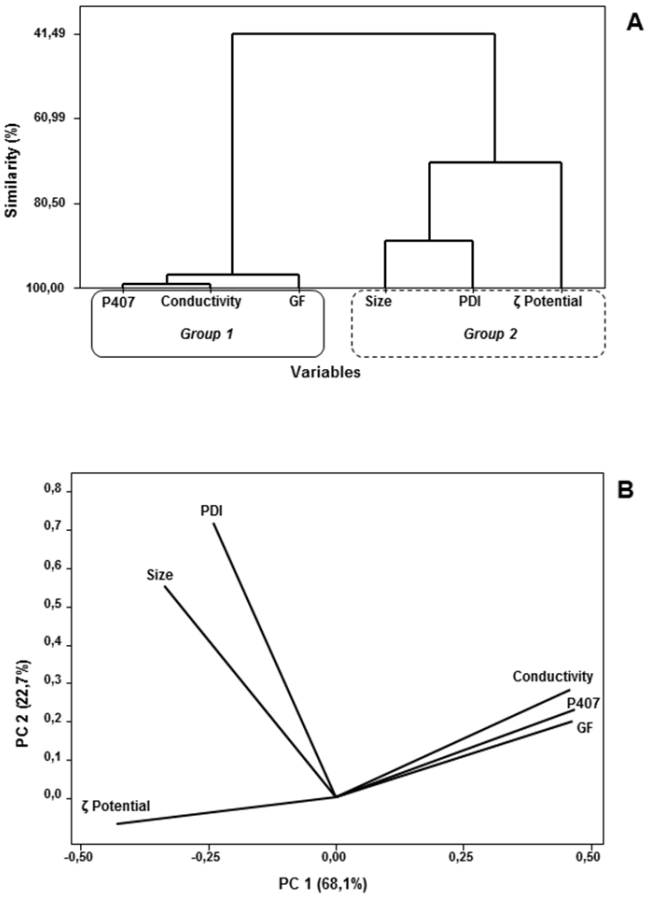


**FIGURE 5 -** HCA and PCA analyses of samples with GF - (A) dendrogram of the GF-P407 mixture samples using the single linkage method and Mahalanobis distance; (B) Loading plots (PC1 versus PC2) from variables. Group 1: P407 (polymer concentration), conductivity, GF solubilized; Group 2: particle size, PDI (polydispersity index), and ζ potential.

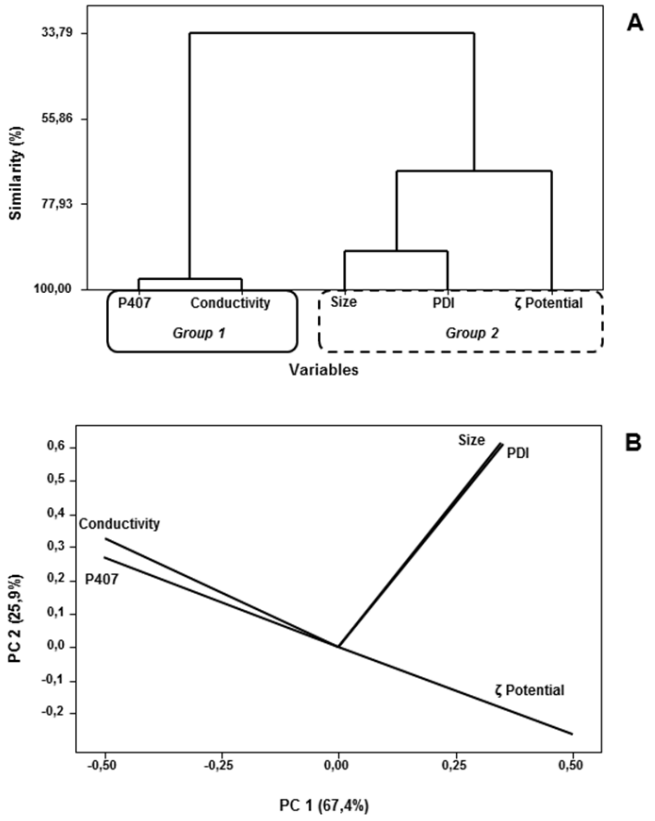


**FIGURE 6 -** HCA and PCA analyses of samples without GF - (A) dendrogram of the P407 samples using the single linkage method and Mahalanobis distance; (B) Loading plots (PC1 versus PC2) from variables. Group 1: P407 (polymer concentration) and conductivity; Group 2: particle size, PDI (polydispersity index), and ζ potential.

## Analysis of GF-P407 interaction via an evaluation of its synthesis impurities

Some of the GF impurities derived from its fermentation or chemical degradation have been identified and described (Townley, 1979; Kahsay *et al.*, 2013). In the present study, these impurities were also observed in the GF sample in the absence of P407. Notably, in the GF solubilization study, changes were noted to occur for the peak area of some impurities as the P407 concentration increased. Thus, the evaluation of a potential GF-P407 interaction was performed by considering the impurity solubilization profile and its structural differences (Figure 7).

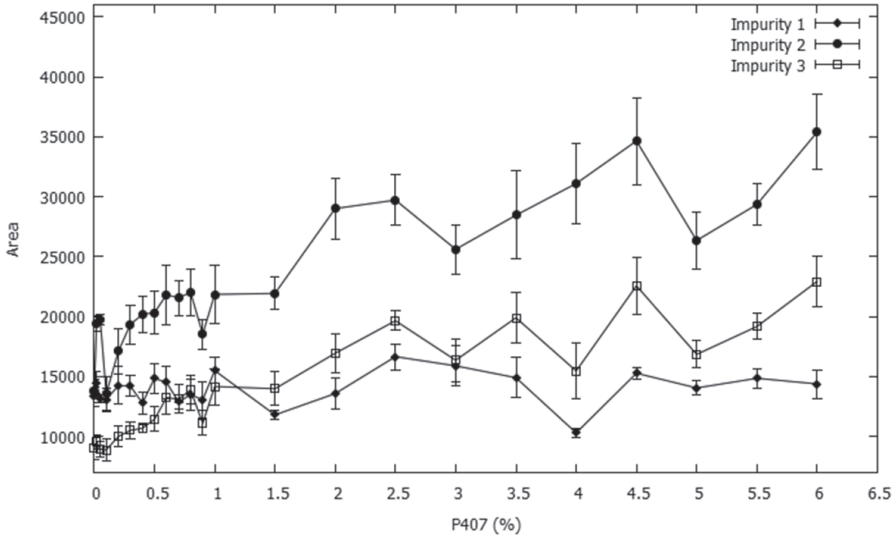


**FIGURE 7 -** Solubilization profile of the GF impurity synthesis/degradation - (Impurity 1: griseofulvinic acid; Impurity 2: dechlorogriseofulvin; Impurity 3: deidrogriseofulvin).

According to Kahsay *et al.* (2013), the main impurities related to GF were griseofulvinic acid (impurity 1), dechlorogriseofulvin (impurity 2), and deidrogriseofulvin (impurity 3) (Figure 8). The solubilization of the impurities, dechlorogriseofulvin and deidrogriseofulvin, revealed a strong correlation with the profile presented for GF ($r_{Pearson}$ 0.9156 and 0.9142, respectively). However, the griseofulvinic acid solubilization was different to GF profile ($r_{Pearson}$ 0.1166), and to dechlorogriseofulvin ($r_{Pearson}$ 0.2286) and deidrogriseofulvin ($r_{Pearson}$ 0.3848) profiles.

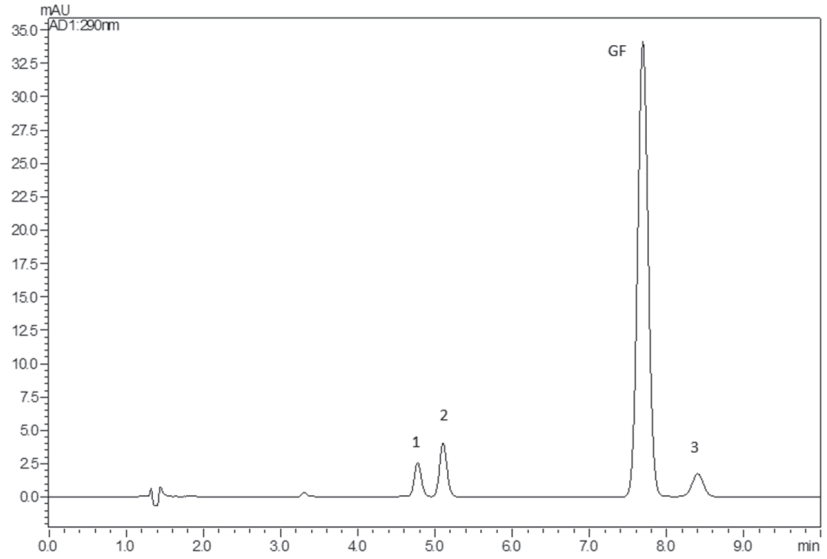


**FIGURE 8 -** GF and impurity chromatogram in the presence of P407 - 1: griseofulvinic acid; 2: dechlorogriseofulvin; GF: griseofulvin; and 3: dechlorogriseofulvin.

Through multivariate analysis, the correlation between the solubilization profiles was confirmed as the HCA and PCA analyses revealed the presence of two groups. GF, dechlorogriseofulvin, and deidrogriseofulvin constitute the first group, with similar solubility profiles. Griseofulvin acid is composed of the second group, demonstrating a different behavior for GF and the other two impurities. In contrast to GF and the other two impurities, the griseofulvinic acid molecule did not exhibit cyclohexene ring unsaturation. In conjunction with the data obtained from the FT-IR and NMR analyses, it is plausible to propose that the increased solubility of GF can be attributed to the interaction between the $sp^2$ unsaturation of GF and P407.

## Fungal susceptibility tests

The fungal susceptibility tests for samples containing GF-P407 association against *Trichophyton mentagrophytes* and *Trichophyton rubrum* isolates showed MIC values ranging from 0.0028 to 0.0172 mM, except for *Trichophyton mentagrophytes* – TME 34, which was not inhibited. For samples containing GF alone, the MIC values against isolates of *T. mentragrophytes* and *T. rubrum* were 0.0028 and 0.0056 mM, respectively (Table I). By comparing the MIC values obtained for GF alone and GF-P407 dispersions, a decrease in drug activity was noted for samples containing P407. This finding is more than evident for *Trichophyton mentagrophytes* – TME 34, which was not susceptible when exposed to a 10-fold higher concentration of the drug with P407 at 4.76 mM. Under the same experimental conditions, P407 showed no antifungal activity at the concentrations tested.

**TABLE I -** MIC values (μg/mL) of GF alone and GF-P407 association sample

| | MIC (μg/mL) | | | | | |
|---|---|---|---|---|---|---|
| **Isolates/Samples** | **GF** | **Sample 1** | **Sample 2** | **Sample 3** | **Sample 4** | **Sample 5** |
| *T. mentragrophytes* | | | | | | |
| TME16 | 1.0 | 1.2 | 1.0 | 1.5 | 1.2 | - |
| TME40 | 1.0 | 1.3 | 1.9 | 1.5 | 2.0 | - |
| TME34 | NI | NI | NI | NI | NI | NI |
| *T. rubrum* | | | | | | |
| TRU51 | 2.0 | 2.6 | 3.8 | 6.2 | 4.0 | - |
| TRU43 | 2.0 | 1.3 | 3.8 | 5.3 | 4.0 | - |

*Sample 1 = 0.5% P407; Sample 2 = 1.0% P407; Sample 3 = 2.0% P407; Sample 4 = 3.0% P407; Sample 5 = 6.0% P407. NI = not inhibition.

To calculate the binding constant or apparent stability constant ($K_S$) between GF and P407, the linear region of the sigmoid solubilization curve was analyzed using a regression model ($y = 0.0511x + 0.000003$; $r^2 = 0.9957$). Subsequently, the $K_S$ value was calculated using equation 1 (Higuchi, Connors, 1965; Brewster, Loftsson, 2007):

$$K_S = \text{Slope} / S_0 (1\text{-Slope}) \quad (1)$$

where $S_0$ is the solubility of GF in the absence of polymer.

The high value observed (2,100 $M^{-1}$) indicates the formation of a stable complex between GF and P407 (Lee, Shin, Oh, 2003; Loftsson, Brewster, 2009; Changdeo *et al.*, 2011; Parmar, Shah, Sheth, 2011). This result might explain the low antifungal activity of GF-P407; this is because GF must be free from the polymer to permeate the fungal membrane and exert its activity on microtubule assembly (Odds, Brown, Gow, 2003).

The formulation with poloxamer 407 resulted in a critical increase in the amount of solubilized GF. Although some techniques enable a higher increase in GF solubility, the advantages of micellar solubilization are far beyond solubilization (Al-Obaidi *et al.*, 2019). Polymeric micelles are also employed to enhance stability and control wetting, bioavailability, and the controlled release of drugs. P407 presents low toxicity, good compatibility with chemical substances and biological media, and allows the development of different pharmaceutical formulations (Torchilin, 2001; Bodratti, Alexandridis, 2018). Different P407 supra-micellar structures could participate in the distinct behavior of GF solubilization, as suggested by the stepped sigmoid shape gained while the polymer amounts were increased. The molecular interaction between the two substances was inferred by physicochemical tests and might involve the cyclohexene ring of GF. Notably, no relationship was observed between the increase in the solubilized amount of griseofulvin and the enhancement of its antifungal activity. In this context, a more detailed approach of the relationship between poloxamer-induced solubilization of GF and the improvement of its therapeutic response might be a reasonable scope for examination, especially in the development of new pharmaceutical forms of GF administration.

## CONFLICT OF INTEREST

The authors declare no conflict of interest.

## ACKNOWLEDGMENTS

The authors are grateful to Brazilian Conselho Nacional de Desenvolvimento Científico e Tecnológico

- CNPq and Coordenação de Aperfeiçoamento de Pessoal de Nível Superior – CAPES (finance code 001) for financial support to conduct this study.

## REFERENCES

Aggarwal N, Shishu G, Khurana R. Formulation, characterization and evaluation of an optimized microemulsion formulation of griseofulvin for topical application. Colloids Surf. B Biointerfaces. 2013;105:158-166.

Aitipamula S, Vangala VR, Chow PS, Tan RBH. Cocrystal hydrate of an antifungal drug, griseofulvin, with promising physicochemical properties. Cryst Growth Des. 2012;12(12):5858-5863.

Alexandridis P, Athanassiou V, Fukuda S, Hatton TA. Surface activity of poly(ethylene oxide)-block-poly(propylene oxide)-block-poly(ethylene oxide) copolymers. Langmuir. 1994;10(8):2604-2612.

Alexandridis P, Olsson U, Lindman B. A record nine different phases (four cubic, two hexagonal, and one lamellar lyotropic liquid crystalline and two micellar solutions) in a ternary isothermal system of an amphiphilic block copolymer and selective solvents (water and oil). Langmuir. 1998;14(10):2627-2638.

Aly R, Bayles CI, Oakes RA, Bibel DJ, Maibach HI. Topical griseofulvin in the treatment of dermatophytoses. Clin Exp Dermatol. 1994;19(1):43-46.

Al-Obaidi H, Kowalczyk RM, Kalgudi R, Zariwala MG. Griseofulvin solvate solid dispersions with synergistic effect against fungal biofilms. Colloids Surf. B. 2019;184:1-10.

Amidon GL, Lennernäs H, Shah VP, Crison JR. A theoretical basis for a biopharmaceutic drug classification: the correlation of in vitro drug product dissolution and in vivo bioavailability. Pharm Res. 1995;12(3):413-420.

Arida AI, Al-Tabakha MM, Hamoury HAJ. Improving the high variable bioavailability of griseofulvin by SEDDS. Chem Pharm Bull. 2007;55(12):1713-1719.

Bodratti AM, Alexandridis P. Formulation of Poloxamers for Drug Delivery. J Funct Biomater. 2018;9(11):1-24.

Buckley ST, Frank KJ, Fricker G, Brandl M. Biopharmaceutical classification of poorly soluble drugs with respect to ‘‘enabling formulations’’. Eur J Pharm Sci. 2013;50(1):8-16.

Chen Y, Liu C, Chen Z, Su C, Hageman M, Hussain M, et al. Drug-polymer-water interaction and its implication for the dissolution performance of amorphous solid dispersions. Mol Pharm. 2015;12(2):576-589.

Chiappetta DA, Facorro G, Celis ER, Sosnik A. Synergistic encapsulation of the anti-HIV agent efavirenz within mixed poloxamine/poloxamer polymeric micelles. Nanomedicine: NBM. 2011;7(5):624-637.

Dhanaraju MD, Kumaran KS, Baskaran T, Moorthy MSR. Enhancement of bioavailability of griseofulvin by its complexation with β-cyclodextrin. Drug Dev Ind Pharm. 1998;24(6):583-587.

Dumortier G, Grossiord JL, Agnely F, Chaumeil JC. A Review of Poloxamer 407 Pharmaceutical and Pharmacological Characteristics. Pharm Res. 2006;23(12):2709-2728.

Feng T, Pinal R, Carvajal MT. Process induced disorder in crystalline materials: differentiating defective crystals from the amorphous form of griseofulvin. J Pharm Sci. 2008;97(8):3207-21.

Finkelstein E, Amichai B, Grunwald MH. Griseofulvin and its uses. Int J Antimicrob Agents. 1996;6(4):189-194.

Fujioka Y, Kadono K, Fujie Y, Metsugi Y, Ogawara K, Higaki K, et al. Prediction of oral absorption of griseofulvin, a BCS class II drug, based on GITA model: Utilization of a more suitable medium for *in-vitro* dissolution study. J Control Release. 2007;119(2):222-228.

Garg RK, Sachdeva RK, Kapoor G. Comparison of crystalline and amorphous carriers to improve the dissolution profile of water insoluble drug itraconazole. Int J Pharm Bio Sci. 2013;4(1):934-948.

Ghaffari S, Varshosaz J, Saadat A, Atyabi F. Stability and antimicrobial effect of amikacin-loaded solid lipid nanoparticles. Int J Nanomed. 2011;6:35-43.

Gupta AK, Mays RR, Versteeg SG, Piraccini BM, Shear NH, Piguet V, et al. Tinea capitis in children: a systematic review of management. J Eur Acad Dermatol Venereol. 2018;32(12):2264-2274.

Ivanova R, Lindman B, Alexandridis P. Effect of glycols on the self-assembly of amphiphilic block copolymers in water. 1. Phase diagrams and structure identification. Langmuir. 2000a;16(8):3660-3675.

Ivanova R, Lindman B, Alexandridis P. Evolution in structural polymorphism of pluronic F127 Poly(ethyleneoxide)-Poly(propyleneoxide) block copolymer in ternary systems with water and pharmaceutically acceptable organic solvents: from “Glycols” to “Oils”. Langmuir. 2000b;16(23):9058-9069.

Kabanov AV, Alakhov VY. Pluronic® Block Copolymers in Drug Delivery: from Micellar Nanocontainers to Biological Response Modifiers. Crit Rev Ther Drug. 2002;19(1):1-73.

Kahsay G, Adegoke AO, Van Schepdael A, Adams E. Development and validation of a reversed phase liquid

chromatographic method for analysis of griseofulvin and impurities. J Pharm Biomed Anal. 2013;80:9-17.

Kawabata Y, Wada K, Nakatani M, Yamada S, Onoue S. Formulation design for poorly water-soluble drugs based on biopharmaceutics classification system: Basic approaches and practical applications. Int J Pharm. 2011;420(1):1-10.

Khadka P, Ro J, Kim H, Kim I, Kim JT, Kim H, et al. Pharmaceutical particle technologies: An approach to improve drug solubility, dissolution and bioavailability. Asian J Pharm Sci. 2014;9(6):304-316.

Kim EJ, Chun MK, Jang JS, Lee IH, Lee KR, Choi HK. Preparation of a solid dispersion of felodipine using a solvent wetting method. Eur J Pharm Biopharm. 2006;64(2):200–205.

Lau BK, Wang Q, Sun W, Li L. Micellization to gelationof a triblock copolymer in water: Thermoreversibility and scaling. J Polym Sci B Polym Phys. 2004;42(10):2014-2025.

Lawrence MJ. Surfactant Systems: Their use in drug delivery. Chem Soc Rev. 1994;(6):417-424.

Lee KR, Kim EJ, Seo SW, Choi HK. Effect of Poloxamer on the Dissolution of Felodipine and Preparation of Controlled Release Matrix Tablets Containing Felodipine. Arch Pharm Res. 2008;31(8):1023-1028.

Lee K, Shin SC, Oh I. Fluorescence Spectroscopy Studies on Micellization of Poloxamer 407 Solution. Arch Pharm Res. 2003;26(8):653-658.

Lin Y, Alexandridis P. Temperature-dependent adsorption of pluronic F127 block copolymers onto carbon black particles dispersed in aqueous media. J Phys Chem B. 2002;106(42):10834-10844.

Liveri MLT, Licciardi M, Sciascia L, Giammona G, Cavallaro G. Peculiar mechanism of solubilization of a sparingly water soluble drug into polymeric micelles. Kinetic and Equilibrium Studies. J Phys Chem B. 2012;116(16):5037-5046.

Mortensen K. Structural properties of self-assembled polymeric aggregates in aqueous solutions. Polym Adv Technol. 2001;12(1-2):2-22.

Noomen A, Hbaieb S, Parrot-Lopez H, Kalfat R, Hatem F, Amdouni N, et al. Emulsions of β-cyclodextrins grafted to silicone for the transport of antifungal drugs. Mater Sci Eng C. 2008;28(5-6):705-715.

Odds FC, Brown AJP, Gow, NAR. Antifungal agents: mechanisms of action. TRENDS Microbiol. 2003;11(6):272-279.

Oliveira CP, Ribeiro MENP, Ricardo NMPS, Souza TVP, Moura CL, Chaibundit C, et al. The effect of water-soluble polymers, PEG and PVP, on the solubilisation of griseofulvin in aqueous micellar solutions of Pluronic F127. Int J Pharm. 2011;421(2):252-257.

Rekatas CJ, Mai SM, Crothers M, Quinn M, Collet JH, Attwood D, et al. The effect of hydrophobe chemical structure and chain length on the solubilization of griseofulvin in aqueous micellar solutions of block copoly(oxyalkylene)s. Phys Chem Chem Phys. 2001;3(21):4769-4773.

Ren J, Fang Z, Yao L, Dahmani FZ, Yin L, Zhou J, et al. A micelle-like structure of poloxamer–methotrexate conjugates as nanocarrier for methotrexate delivery. Int J Pharm. 2015;487(1-2):177-186.

Ribeiro MENP, Cavalcante IM, Ricardo NMPS, Mai SM, Attwood D, Yeates SG, Booth C. Solubilisation of griseofulvin in aqueous micellar solutions of diblock copolymers of ethylene oxide and 1,2-butylene oxide with lengthy B-blocks. Int J Pharm. 2009;369(1-2):196-198.

Rowe R, Sheskey P, Owen S. Pharmaceutical Handbook of Pharmaceutical Excipients, 5th ed. London: Pharmaceutical Press; 2005.

Sezgin Z, Yüksel N, Baykara T. Preparation and characterization of polymeric micelles for solubilization of poorly soluble anticancer drugs. Eur J Pharm Biopharm. 2006;64(3):261-268.

Shishu G, Aggarwal N. Preparation of hydrogels of griseofulvin for dermal application. Int J Pharm. 2006;326(1-2):20-24.

Suksiriworapong J, Rungvimolsin T, A-gomol A, Junyaprasert VB, Chantasart D. Development and Characterization of Lyophilized Diazepam-Loaded Polymeric Micelles. AAPS PharmSciTech. 2014;15(1):52-64.

Takagi T, Ramachandran C, Bermejo M, Yamashita S, Yu LX, Amidon GL. A Provisional Biopharmaceutical Classification of the Top 200 Oral Drug Products in the United States, Great Britain, Spain, and Japan. Mol Pharm. 2006;3(6):631-643.

Torchilin VP. Structure and design of polymeric surfactant-based drug delivery systems. J Control Release. 2001;73(2-3):137–172.

Townley ER. Griseofulvin, in: K. Florey, editor. Analytical Profiles of Drug Substances. New York: Academic Press; 1979. p. 219–249.

Received for publication on 06th September 2019
Accepted for publication on 29th May 2020